First-principles study on the geometric and electronic structures and phase transition of $PbZr_{1-x}Ti_xO_3$ solid solutions*

Liu Shi-Yu(刘士余)[a)†], Shao Qing-Sheng(邵庆生)[a)], Yu Da-Shu(余大书)[a)], Lü Yue-Kai(吕跃凯)[a)], Li De-Jun(李德军)[a)], Li Yong(李 雍)[b)], and Cao Mao-Sheng(曹茂盛)[b)‡]

[a)] *College of Physics and Electronic Information, Tianjin Normal University, Tianjin* 300387, *China*
[b)] *College of Materials Science and Engineering, Beijing Institute of Technology, Beijing* 100081, *China*

(Received 28 May 2012; revised manuscript received 26 June 2012)

With first-principles virtual-crystal approximation calculations, we systematically investigate the geometric and electronic structures as well as the phase transition of lead zirconate titanate ($PbZr_{1-x}Ti_xO_3$ or PZT) as a function of Ti content for the whole range of $0 \leq x_{Ti} \leq 1$. It can be found that, with the increase of the Ti content, the $PbZr_{1-x}Ti_xO_3$ solid solutions undergo a rhombohedral-to-tetragonal phase transition, which is consistent with the experimental results. In addition, we also show the evolution in geometric and electronic structures of rhombohedral and tetragonal $PbZr_{1-x}Ti_xO_3$ with the increasing content of Ti.

Keywords: PZT, phase transition, density functional theory

PACS: 77.55.hj, 64.60.Ej, 71.15.Mb **DOI:** 10.1088/1674-1056/22/1/017702

1. Introduction

Although lead-free piezoelectric ceramics are developing rapidly at present due to their environmentally friendly nature,[1,2] few of them can match the lead zirconate titanate based ceramics with excellent properties. The lead zirconate titanate ($PbZr_{1-x}Ti_xO_3$ or PZT) based ceramics are widely used in electronic devices and in other technological applications due to their piezoelectric, ferroelectric, and dielectric properties.[3–5] The $PbZr_{1-x}Ti_xO_3$ is a well-known continuous solid solution of both $PbZrO_3$ and $PbTiO_3$, whereas neither ferroelectric $PbTiO_3$ nor antiferroelectric $PbZrO_3$ are particularly good piezoelectrics. However, the solid solution prepared using these materials gives rise to an excellent piezoelectric response, which attracts much attention from the experimental researchers.[6–11]

The macroscopic phase of $PbZr_{1-x}Ti_xO_3$ depends on the Zr/Ti content ratio and temperature. The $PbZr_{1-x}Ti_xO_3$ phase diagram given by Jaffe *et al.*,[12] which only covers temperatures above 300 K, has been accepted as the basic characterization of the PZT solid solution. This solid solution is cubic at high temperatures, but it becomes slightly distorted at lower temperatures, where it is ferroelectric. Except for a narrow region close to $PbZrO_3$, the ferroelectric region of the PZT phase diagram consists mainly of a Zr-rich rhombohedral (*R*3*m* at high temperature and *R*3*c* at low temperature) region and Ti-rich tetragonal (space group *P*4*mm*) region. Piezoelectric solid solutions $PbZr_{1-x}Ti_xO_3$ undergo a rhombohedral-to-tetragonal phase transition with the increasing content of Ti.[12,13] A nearly vertical phase boundary between the rhombohedral and tetragonal regions of the phase diagram close to $x = 0.5$ is defined as the morphotropic phase boundary (MPB), where the material displays the highest values of the dielectric and electromechanical constants.[12,13]

To the best of our knowledge, the detailed evolution of the structures, the electronic properties and the phase transition of the $PbZr_{1-x}Ti_xO_3$ as a function of Ti content for the whole range of $0 \leq x_{Ti} \leq 1$ is still unclear on the atomic level, due to the lack of single crystals with high quality for a significant part of the PZT phase diagram.[14] As is well known, the first-principles calculation based on the density functional theory is a popular theoretical tool for studying solid materials.[15–20] Here, we present a study on the atomic and electronic structures as well as phase transition of $PbZr_{1-x}Ti_xO_3$ as a function of Ti content by first-principles virtual-crystal approximation (VCA) calculations.

2. Calculation model and method

The first-principles calculations were based on density functional theory (DFT), VCA, pseudopotential method, and plane-wave basis sets.[21–23] The results reported in this paper were obtained by using the Cambridge serial total energy package (CASTEP).[24] The electronic configurations of the Pb, Ti, Zr, and O atoms in the ground state used in the ultrasoft pseudopotentials were $[Xe]4f^{14}5d^{10}6s^26p^2$, $[Ne]3s^23p^63d^24s^2$, $[Ar][3d^{10}]4s^24p^64d^25s^2$, and $[1s^2]2s^22p^4$, respectively. The exchange-correlation effects were treated

*Project supported by the National Natural Science Foundation of China (Grant Nos. 11104203, 11075116, 50972014, 51072024, and 51132002) and the Foundation of Introduction of Talent of Tianjin Normal University, China (Grant No. 5RL100).

†Corresponding author. E-mail: buaasyliu@gmail.com
‡Corresponding author. E-mail: caomaosheng@bit.edu.cn

© 2013 Chinese Physical Society and IOP Publishing Ltd

with the generalized gradient approximation (GGA) implemented in the Perdew–Burke–Ernzerhof (PBE) scheme.[25]

To model the quaternary $PbZr_{1-x}Ti_xO_3$ ($0 \leq x_{Ti} \leq 1$) solid solutions of the generic composition, we have adopted the VCA, which implies preserving the same crystalline unit cells as the ternary compounds such as $PbTiO_3$ and replacing the transition metal Ti with a virtual Zr atom.[26] The crystal structures of tetragonal and rhombohedral *R*3*m* and *R*3*c* $PbZr_{1-x}Ti_xO_3$ phases are shown in Fig. 1. A plane-wave cutoff energy of 400 eV was employed in the calculations, which assured a total energy convergence of 10^{-6} eV per atom. For the bulk calculations in which primitive unit cells were employed, the Brillouin zone sampling was set with the $8 \times 8 \times 8$ Monkhorst–Pack *k*-points meshes.[27] All the primitive unit cells were allowed to fully relax until the force on each atom was smaller than 0.01 eV/Å. Our GGA calculations yielded lattice constants of $a = 3.895$ Å and $c = 4.134$ Å for tetragonal $PbTiO_3$ bulk and $a = 5.877$ Å for rhombohedral $PbZrO_3$ bulk with *R*3*c* structure, respectively, which agree well with the experimental data and previous DFT–GGA calculations.[28–30]

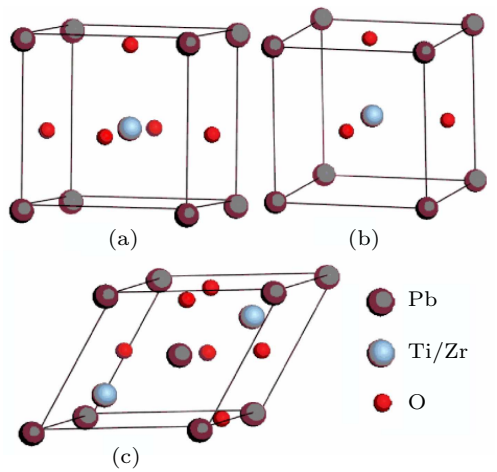


Fig. 1. Crystal structures of $PbZr_{1-x}Ti_xO_3$: (a) tetragonal, (b) *R*3*m*, and (c) *R*3*c*.

3. Results and discussion

3.1. Energetics and phase transition

Figure 2 shows the total energy differences of the $PbZr_{1-x}Ti_xO_3$ with rhombohedral (E_{R3m}, E_{R3c}) and tetragonal (E_{tetra}) structures as a function of Ti content for the whole range of $0 \leq x_{Ti} \leq 1$. The total energy of the rhombohedral $PbZr_{1-x}Ti_xO_3$ is found to be lower than that of the tetragonal $PbZr_{1-x}Ti_xO_3$ for a low content of Ti, which indicates that the rhombohedral $PbZr_{1-x}Ti_xO_3$ is more stable under the Ti-poor (Zr-rich) condition. When the content of Ti increases, however, the total energy of the tetragonal $PbZr_{1-x}Ti_xO_3$ gradually becomes lower than that of the rhombohedral $PbZr_{1-x}Ti_xO_3$. Thus, under the Ti-rich condition, the tetragonal $PbZr_{1-x}Ti_xO_3$ is more stable than the rhombohedral $PbZr_{1-x}Ti_xO_3$. All of the above predictions are consistent with the experimental results.[12,13]

Furthermore, we can see from Fig. 2 that, the rhombohedral $PbZr_{1-x}Ti_xO_3$ is more stable than the tetragonal $PbZr_{1-x}Ti_xO_3$ in the range of $0 < x_{Ti} < 0.6$, while tetragonal $PbZr_{1-x}Ti_xO_3$ is favorable in the range of $0.6 < x_{Ti} < 1$. For the content of $x_{Ti} = 0.6$, the rhombohedral and tetragonal $PbZr_{1-x}Ti_xO_3$ is almost equally stable. Thus, we suggest that the rhombohedral -to -tetragonal phase transition occurs at the composition of $x_{Ti} = 0.6$, which is consistent with the experimental rhombohedral-to-tetragonal phase transition results.[12,13] At $T = 0$ K, the value of phase transition point with $x_{Ti} = 0.6$ obtained by our calculation is slightly higher than the experimental value of phase transition point with $x_{Ti} \approx 0.5$ at room temperature due to the difference in temperature, but the whole tendency of phase transition agrees with the experimental results.[12,13]

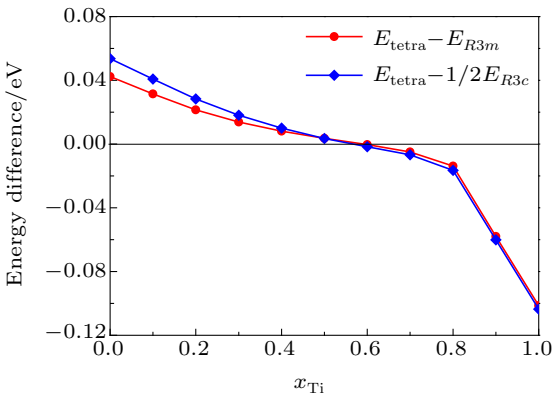


Fig. 2. Total energy differences of the $PbZr_{1-x}Ti_xO_3$ with rhombohedral and tetragonal structures as a function of Ti content for the whole range of $0 \leq x_{Ti} \leq 1$.

3.2. Geometric structure

Figure 3 shows the lattice parameters and volumes of rhombohedral and tetragonal $PbZr_{1-x}Ti_xO_3$ as a function of Ti content for the whole range of $0 \leq x_{Ti} \leq 1$. In Fig. 3(a), the lattice parameters of the rhombohedral *R*3*m* and *R*3*c* $PbZr_{1-x}Ti_xO_3$ decrease with the increasing content of Ti. The lattice parameter *a* of the tetragonal $PbZr_{1-x}Ti_xO_3$ decreases with the increasing content of Ti. However, the lattice parameter *c* of tetragonal $PbZr_{1-x}Ti_xO_3$ decreases with the increasing content of Ti at first, then increases with the increasing content of Ti under Ti-rich conditions. In addition, the lattice constant *a* of *R*3*m* and *R*3*c* structures is just between the lattice constants *a* and *c* of tetragonal structure.

From Fig. 3(b) one can see that the volumes (*V*) of the rhombohedral and tetragonal $PbZr_{1-x}Ti_xO_3$ decrease with the increasing content of Ti. The volume of the rhombohedral *R*3*c* $PbZr_{1-x}Ti_xO_3$ is found to be smaller than that of the rhombohedral *R*3*m* and tetragonal $PbZr_{1-x}Ti_xO_3$ for the whole content of Ti. The volume of the rhombohedral *R*3*m*

$PbZr_{1-x}Ti_xO_3$ is found to be larger than that of the tetragonal $PbZr_{1-x}Ti_xO_3$ for a low content of Ti. When the content of Ti increases, however, the volume of the tetragonal $PbZr_{1-x}Ti_xO_3$ becomes larger than that of the rhombohedral *R*3*m* $PbZr_{1-x}Ti_xO_3$ under Ti-rich conditions.

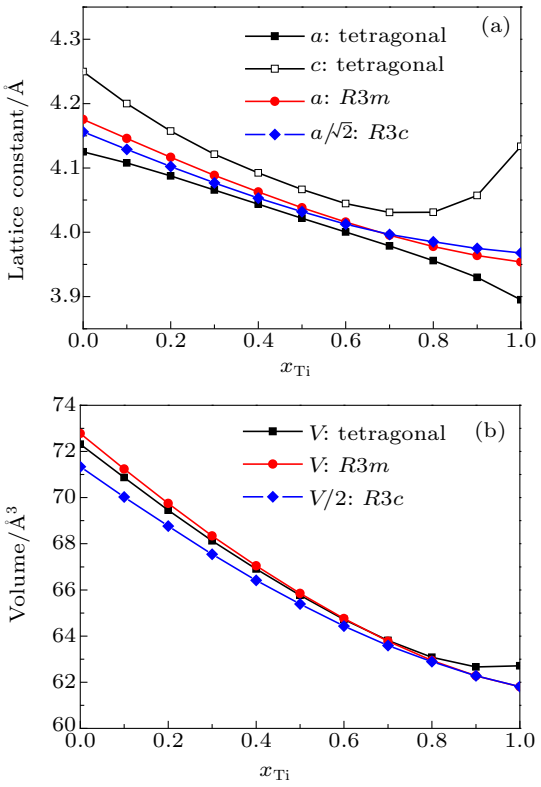


Fig. 3. Lattice parameters (a) and volume (b) of $PbZr_{1-x}Ti_xO_3$ with rhombohedral and tetragonal structures as a function of Ti content for the whole range of $0 \le x_{Ti} \le 1$.

3.3. Electronic structure

In order to elucidate the electronic properties of $PbZr_{1-x}Ti_xO_3$, we calculated their electronic total density of states (TDOS) and band gap (E_g). Figure 4 shows the total DOS curves of tetragonal and rhombohedral *R*3*m* and *R*3*c* $PbZr_{1-x}Ti_xO_3$ structures with $x_{Ti} = 0$, 0.2, 0.4, 0.6, 0.8, and 1. These curves demonstrate that the tetragonal and rhombohedral *R*3*m* and *R*3*c* $PbZr_{1-x}Ti_xO_3$ solid solutions are insulators. It can be seen clearly from Fig. 4 that the TDOS curves of tetragonal and rhombohedral *R*3*m* and *R*3*c* $PbZr_{1-x}Ti_xO_3$ at both −15.7 eV and 5.5 eV are separated into two peaks with the increasing content of Ti. Furthermore, we compare the TDOS of the tetragonal and rhombohedral *R*3*m* and *R*3*c* $PbZr_{1-x}Ti_xO_3$ for the same content of Ti. Under a very low content of Ti, the small peak of TDOS of the rhombohedral $PbZr_{1-x}Ti_xO_3$ on the deep energy level of −16.3 eV is higher than that of the tetragonal one, and the TDOS of the rhombohedral $PbZr_{1-x}Ti_xO_3$ at −1.0 eV shifts downwards (left) relative to the tetragonal one, which indicates the rhombohedral $PbZr_{1-x}Ti_xO_3$ is more stable under the Ti-poor condition. With the increasing content of Ti, the above two characteristics disappear gradually. While under very high content of Ti, it can be seen that the small peak of TDOS of the tetragonal $PbZr_{1-x}Ti_xO_3$ on the low energy level of −3.5 eV is higher than that of the rhombohedral one, which implies the tetragonal $PbZr_{1-x}Ti_xO_3$ is more stable under the Ti-rich condition. These are also consistent with the above results of energetic stability and phase transition.

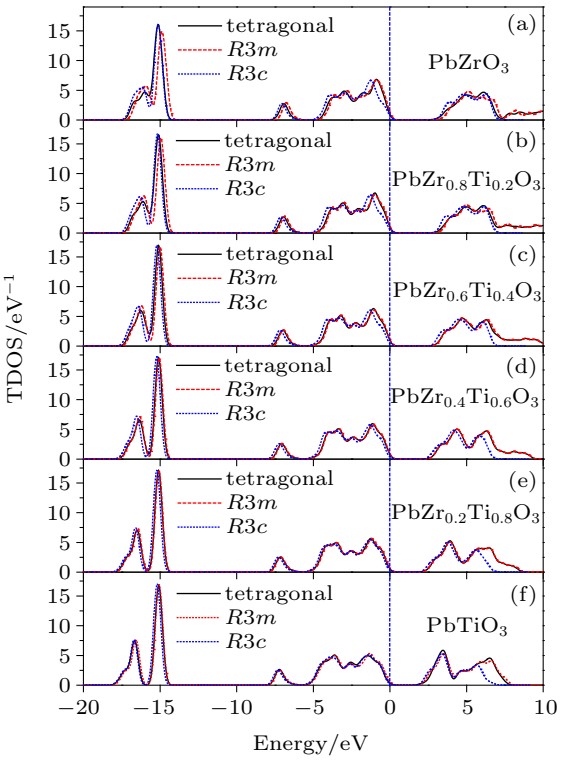


Fig. 4. Total DOS of $PbZr_{1-x}Ti_xO_3$ with tetragonal and rhombohedral structures as a function of Ti content for (a)–(f) $x_{Ti} = 0$, 0.2, 0.4, 0.6, 0.8, and 1.

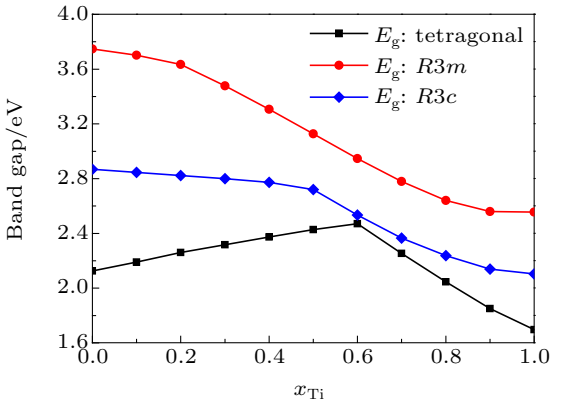


Fig. 5. Band gap of $PbZr_{1-x}Ti_xO_3$ with rhombohedral and tetragonal structures as a function of Ti content for the whole range of $0 \le x_{Ti} \le 1$.

Figure 5 shows the band gap of $PbZr_{1-x}Ti_xO_3$ with rhombohedral and tetragonal structures as a function of Ti content for a range of $0 \le x_{Ti} \le 1$. In the whole view, the band gap of rhombohedral $PbZr_{1-x}Ti_xO_3$ with *R*3*m* structure is the largest, while the band gap of the tetragonal one is the smallest. The

band gap of rhombohedral $PbZr_{1-x}Ti_xO_3$ with $R3c$ structure is just between them. Furthermore, we can see that the band gaps of the rhombohedral $R3m$ and $R3c$ $PbZr_{1-x}Ti_xO_3$ decrease with the increasing content of Ti. However, the band gap of tetragonal $PbZr_{1-x}Ti_xO_3$ increases with the increasing content of Ti up to $x_{Ti} = 0.6$, then it decreases with the increasing content of Ti. Moreover, it can also be found that the transition point of the band gap at $x_{Ti} = 0.6$ is near the calculated point of phase transition, and the band gap of the tetragonal and rhombohedral $R3m$ structure is almost equal at this point.

4. Conclusion

In summary, we have systematically investigated the structure and phase transition of lead zirconate titanate $PbZr_{1-x}Ti_xO_3$ (PZT) as a function of Ti content for the whole range of $0 \leq x_{Ti} \leq 1$ by first-principles virtual-crystal approximation (VCA) calculations. Our results show that a compositional phase transition of $PbZr_{1-x}Ti_xO_3$ occurs from the Zr-rich rhombohedral phase to the Ti-rich tetragonal phase with the increasing Ti content, which is consistent with the experimental results. In this process of rhombohedral-to-tetragonal phase transition, we find that the volume and band gap decrease gradually with the increasing content of Ti.

References

[1] Tian X X, Qu S B, Du H L, Li Y and Xu Z 2012 *Chin. Phys.* B **21** 037701

[2] Zhao J B, Du H L, Qu S B, Zhang H M and Xu Z 2011 *Chin. Phys.* B **20** 067701

[3] Uchino K 1971 *Piezoelectric Actuators and Ultrasonic Motors* (Dordrecht: Kluwer)

[4] Cross E 2004 *Nature* **432** 24

[5] Chen Z J, Zheng J A, Zhang S Y, Mi X B and Zheng K 2010 *Chin. Phys.* B **19** 118104

[6] Lin H B, Cao M S, Yuan J, Wang D W, Zhao Q L and Wang F C 2008 *Chin. Phys.* B **17** 4323

[7] Liu H M, Zhao Q L, Cao M S, Yuan J, Duan Z X and Qiu C J 2008 *Chin. Phys. Lett.* **25** 4128

[8] Zhang D Q, Wang D W, Yuan J, Zhao Q L, Wang Z Y and Cao M S 2008 *Chin. Phys. Lett.* **25** 4410

[9] Wang D W, Zhang D Q, Yuan J, Zhao Q L, Liu H M, Wang Z Y and Cao M S 2009 *Chin. Phys.* B **18** 2596

[10] Wang D W, Jin H B, Yuan J, Wen B L, Zhao Q L, Zhang D Q and Cao M S 2010 *Chin. Phys. Lett.* **27** 047701

[11] Wang D W, Cao M S, Yuan J, Zhao Q L, Li H B, Zhang D Q and Agathopoulos S 2011 *J. Am. Ceram. Soc.* **94** 647

[12] Jaffe B, Cook W R and Jaffe H 1971 *Piezoelectric Ceramics* (London-New York: Academic Press)

[13] Noheda B 2002 *Curr. Opin. Solid State Mater. Sci.* **6** 27

[14] Clarke R and Whatmore R W 1976 *J. Cryst. Growth* **33** 29

[15] Xu Y J Z, Shang J X and Wang F H 2011 *Chin. Phys.* B **20** 037101

[16] Liu Z H and Shang J X 2012 *Chin. Phys.* B **21** 016202

[17] Lu Z S, Ma D W, Zhang J, Xu G L and Yang Z X 2012 *Chin. Phys.* B **21** 047505

[18] Li M, Zhang J Y, Zhang Y and Wang T M 2012 *Chin. Phys.* B **21** 067302

[19] Wang Y J, Wang C Y and Wang S Y 2011 *Chin. Phys.* B **20** 036801

[20] Liu S Y, Shang J X, Wang F H, Liu S, Zhang Y and Xu H B 2009 *Phys. Rev.* B **80** 085414

[21] Hohenberg P and Kohn W 1964 *Phys. Rev.* **136B** 864

[22] Kohn W and Sham L J 1965 *Phys. Rev.* **140A** 1133

[23] Vanderbilt D 1990 *Phys. Rev.* B **41** 7892

[24] Segall M D, Lindan P L D, Probert M J, Pickard C J, Hasnip P J, Clark S J and Payne M C 2002 *J. Phys. Condens. Matter* **14** 2717

[25] Perdew J P, Burke K and Ernzerhof M 1996 *Phys. Rev. Lett.* **77** 3865

[26] Shao Q S, Liu S Y, Zhao H, Yu D S and Cao M S 2012 *Acta Phys. Sin.* **61** 047103 (in Chinese)

[27] Monkhorst H J and Pack J D 1976 *Phys. Rev.* B **13** 5188

[28] Kuroiwa Y, Aoyagi S, Sawada A, Harada J, Nishibori E, Takata M and Sakata M 2001 *Phys. Rev. Lett.* **87** 217601

[29] Alahmed Z and Fu X H 2007 *Phys. Rev.* B **76** 224101

[30] Kagimura R and Singh D J 2008 *Phys. Rev.* B **77** 104113